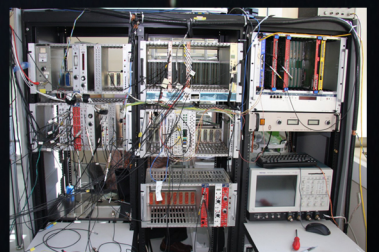
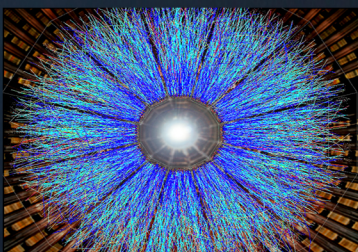


A three weeks experience in the "crazy" world of scientific research ...



Exploring the world of research



Exploring the world of research

@2010 NIHAM, NIPNE, Magurele, Romania

<http://niham.nipne.ro>

Printed in Magurele

Students	Subjects	Tutors
Dorin Cononenco	CBM – TRD	Asist. Andrei Herghelegiu
Madalina Tarzila	CBM - TRD	Asist. Andrei Herghelegiu
Sebastian Toma	CBM – RPC	Dr. Simion Victor
Cristian Vlad	CBM – RPC	Dr. Simion Victor
Ioana Petrescu	MBS – DAQ	Dr. Vasile Catanescu Dr. Florin Constantin
Alexandru Stanculescu	MBS – DAQ	Dr. Vasile Catanescu Dr. Florin Constantin
Mihai Puscas	ALICE-TRD reconstruction	Dr. Alexandru Bercuci

Table of contents

1. Transition Radiation Detector	1
-Dorin Cononenco-	
2. CBM Double-Sided Transition Radiation Detector.....	5
-Madalina Gabriela Tarzila-	
3. Working principles of RPCs.....	9
-Sebastian Toma-	
4. Bulid-up of an RPC.....	14
-Cristian Vlad-	
5. MBS (Multi-Branch System).....	18
-Ioana Petrescu, Alexandru-Octavian Stanculescu-	
6. ALICE TRD Reconstruction and Visualization.....	25
-Mihai-Marian Puscas-	

CBM Single-Sided Transition Radiation Detector

Dorin Cononenco

Technical University, Bucharest, Romania

1. Introduction

The Compressed Baryonic Matter (CBM) is an experiment designed for the investigation of highly compressed nuclear matter at the future Facility for Antiproton and Ion Research (FAIR) at Gesellschaft für Schwerionenforschung (GSI), Darmstadt, Germany^[1].

A super-dense nuclear matter can be created in the reaction volume of relativistic heavy-ion collisions. The main goal for the study of nucleus–nucleus collisions is the exploration of the phase diagram of Quantum Chromo-Dynamics (QCD).

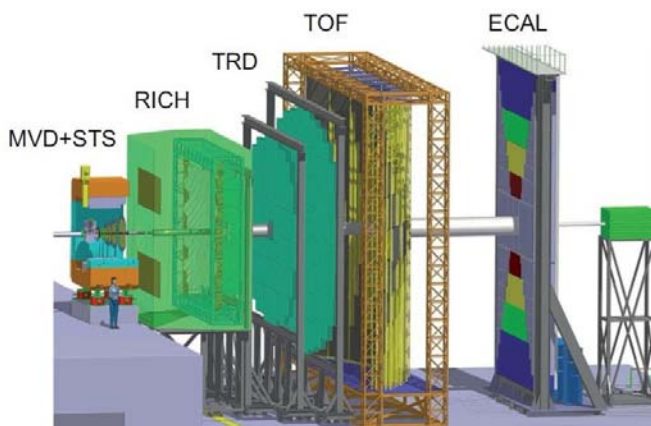


Fig 1 The CBM scheme

The detectors used at the CBM experiment must be able to measure extremely rare signals; this requires very good performances in terms of speed, radiation hardness and granularity.

- The Silicon Tracking System (STS) has to provide the track reconstruction and momentum determination.
- Micro-Vertex Detector (MVD) will be implemented for the determination of primary and secondary vertices with a very high precision.
- the Ring Imaging Cherenkov detector (RICH) provides the electron identification.

- Transition Radiation Detectors (TRD) provides the electron identification and serves as tracking detector for charged particles.^[2]
- the Time-of-Flight (TOF) measurement with a wall of timing Resistive Plate Chambers (RPC) will facilitate the hadron identification.
- Electromagnetic Calorimeter (ECAL) is used for the identification of photons.

The purpose of Transition Radiation Detector (TRD) is to provide electron identification and tracking of all charged particles within the CBM experiment. The expected particle rates for the CBM-TRD detector are up to 10^5 particles/cm²s for 10^7 interactions/s of minimum bias Au+Au collisions at 25 A GeV ^[3].

There are two well known concepts of TRD: the ALICE-TRD - gives very good performance in a high multiplicity environment and at low counting rate - and the ATLAS-TRD - based on straw tubes, with lower granularity but a good performance up to a counting rate of 10^6 particles/cm²s ^[3].

To fulfill the CBM experiment requirements, a high granularity TRD based on a MultiWire Proportional Chamber (MWPC) will be used.

2. Single-sided TRD description

This TRD prototype is composed of a radiator and a MultiWire Proportional Chamber (MWPC), as we see in Fig. 2.

The single-sided CBM-TRD prototype needs a drift region to maximize the absorption probability of the transition radiation generated in the radiator.

In order to discriminate between electrons and pions, the TRD must have a good absorption coefficient of transition radiation (TR) produced by the radiator.

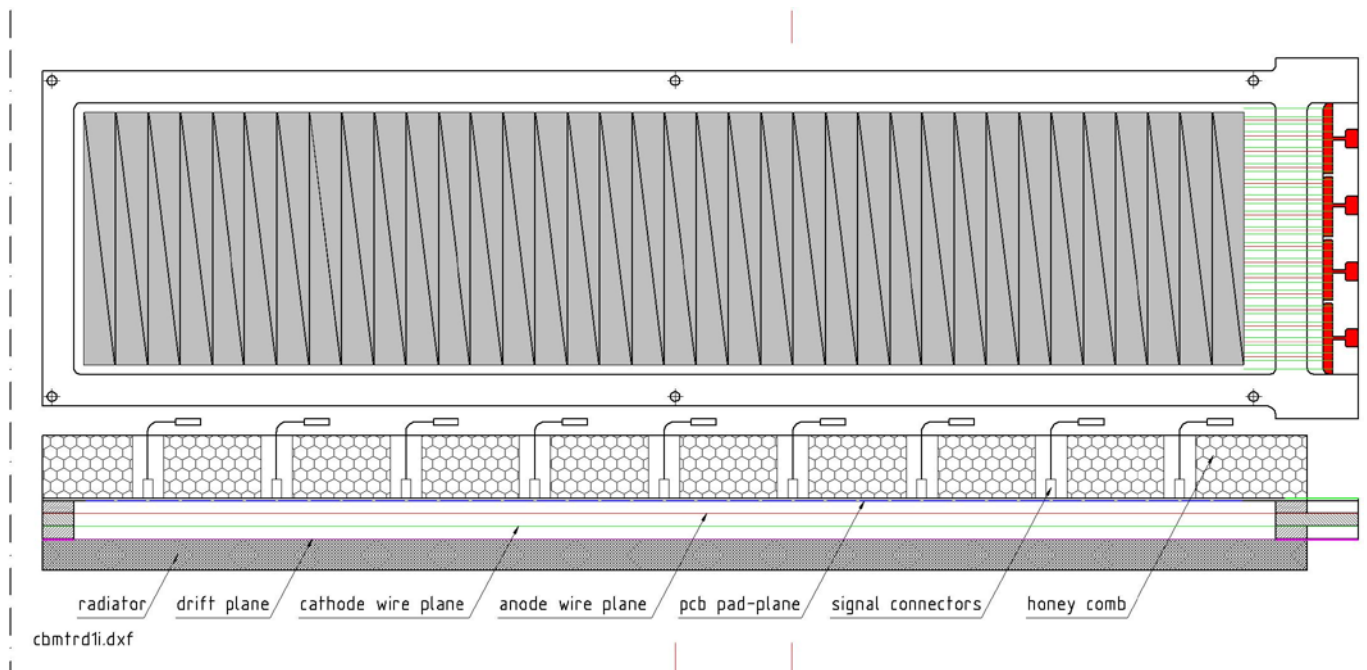


Fig 2. The pad plane design and the cross-section through the detector - perpendicular to the direction of the anode wires.

Transition radiation (a photon with an energy in X-ray range) is produced when an ultra-relativistic charged particle traverses the boundary between materials with different dielectric constants. The probability of photon emission from a single boundary is very small (<1%), so that a large number of boundaries have to be combined to obtain a reasonable efficiency. For this, we use a radiator with a foam structure [4].

The radiator, in which an electron generates the transition radiation (TR), is made out of Rohacell *HF71*, a polymethacrylimide (PMI) foam with low density and high mechanical and chemical stability. The thickness of the radiator in this case is 16mm.

The drift chamber is filled with a gas mixture. In order to maximize the absorption of TR, usually, a gas mixture of Xe (85%) and CO₂ (15%) will be used. The CO₂ gas (nonflammable) is used to reduce the size of the ionization avalanche.

The choice for Xe as the noble gas in the mixture is determined by its large absorption and subsequent ionization of the transition radiation produced in the radiator. Xe is replaced in laboratory tests with Ar with 70% concentration.

The detection chamber can be divided into two regions:

- The drift region, situated between the radiator and cathode wires;
- The amplification region (between cathode wires and cathode pads)[4].

The thickness of the drift region is 4mm and of the amplification region is 8mm (4mm between the cathode wires and anode wires; 4mm between anode wires and cathode pads).

Anode wires (20 μm diameter) are made of Au plated W and the cathode wires (75 μm diameter) made of CuBe alloy. The pitch between anode wires is 3mm and between cathode wires is 1.5 mm.

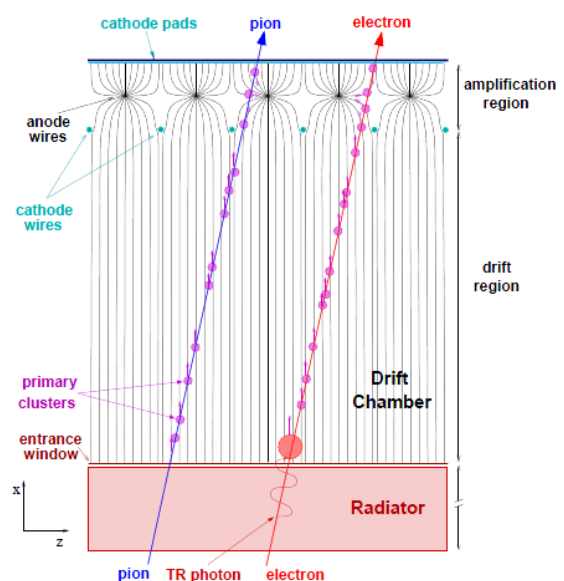


Fig 3 The cross-section through the detector, parallel to the direction of the anode wires for ALICE - TRD.

The readout pad

The MWPC technology offers charged-particle tracking with a good position resolution due to a readout of the cathode which is subdivided into pads providing a high granularity and also determinates the charged particles loss energy in the sensitive chamber volume and may provide a good electron/pion separation. There are 72 triangular Cu pads with the width of 10mm and 80mm height each. The gap between the pads is 0.2mm.

3. Particle Detection

The high-energy particles enter the TRD through the radiator, where they generate the transition radiation and produce ionisations in the gas filled chamber. The radiation created crosses the drift volume where it interacts with gas though the photoelectric effect. The resulted electron will produce secondary ionisations. The electric field is strong enough to drift the freed electrons close to the anode wires, where the strong electric field will accelerate these electrons, and create an ionization avalanche^[4].

The positive ions created in the avalanche process in the vicinity of the anode wire move towards the surrounding electrodes, inducing a positive signal on the pad plane. For a precise determination of the location of the avalanche the pad geometry is optimized in order to have a charge sharing between three adjacent pads. Then the induced charge on the readout pads goes to the preamplifier which creates an electronic signal^[5].

4. Induced charge density distribution

To calculate the induced charge distribution is to use the image charge method.

The formulas used to obtain the charge density distribution:

- for single-sided TRD:

$$\rho(x,y) = \sum_{n=0}^{\infty} \left[\frac{(6n+1)h}{[(6n+1)^2h^2+r^2]^{1.5}} - \frac{(6n+5)h}{[(6n+5)^2h^2+r^2]^{1.5}} \right]$$

- for double-sided TRD:

$$\rho'(x,y) = -\frac{Q_A}{2\pi} \sum_{n=0}^{\infty} (-1)^n \frac{(2n+1)h}{[(2n+1)^2h^2+r^2]^{1.5}}$$

The charge created by the anode avalanche is located between two planes. It is assumed that the induced charge is point-like and is located midway between the two planes separated by a multiple of h , where h is the distance between anode and cathode pads. The induced charge distribution is proportional to the induced electric field at the surface of the cathode plane of interest. This is described by the formulas above ^[6].

The results are presented in Fig. 4.

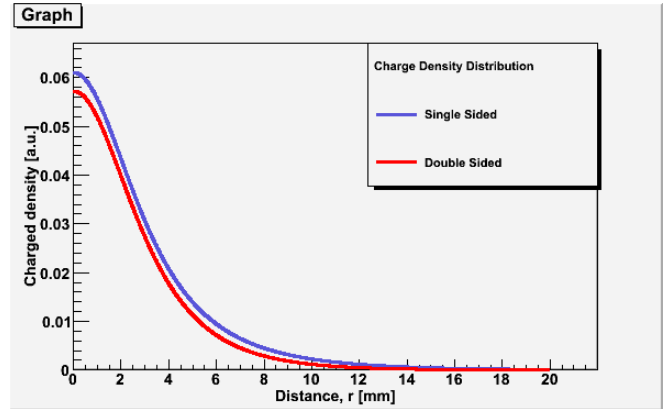


Fig 4. Charge Density Distribution for both TRD geometries – single-sided and double-sided.

The signal on each pad is obtained by integrating the functions in Fig. 4.

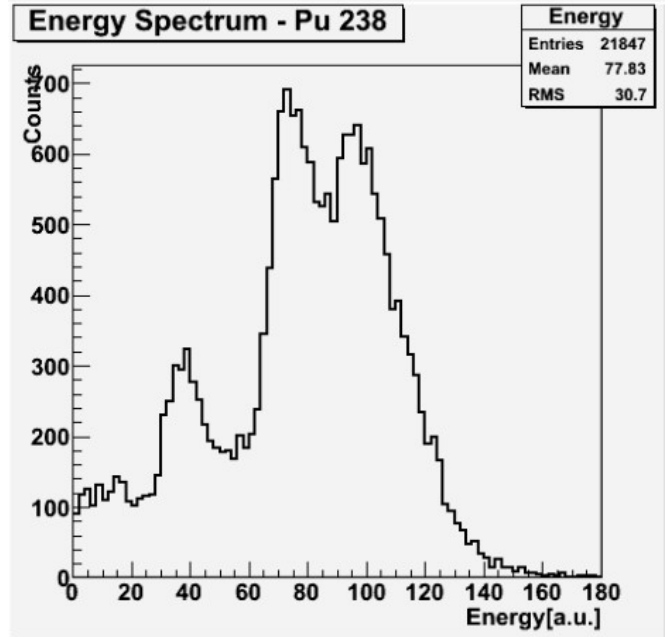


Fig 5. Energy Spectrum for ²³⁸Pu.

The energy spectrum from Fig. 5. was obtained as a charge sum on all readout pads.

The first prototype with the above described geometry was designed and build. Detailed tests using radioactive sources started and tests using beams of e and π are on the way.

5. References

- [1] CBM Tehnical Status Raport GSI, Darmstadt, 2005;
- [2] A.Andronic. The TRD of the CBM experiment, Darmstadt, Germany. Nuclear Instruments and Methods in Physics Research A 563 (2006);
- [3] M.Petris, M.Petrovici et al. High Counting rate transition radiation detector, Nuclear Instruments and Methods in Physics Research A 581 (2007);
- [4] Transition Radiation Detector (TRD). ALICE Technical Design Report. CERN/LHCC 2001-021, 3 October 2001;
- [5] Melanie Klein-Bösing . Development of a Transition Radiation Detector and Reconstruction of Photon Conversions in the CBM Experiment . , 2009, PhD Thesis
- [6] Bo Yu, Gas proportional detectors with interpolating cathod pad readout for high track multiplicities, December 1991

CBM Double-Sided Transition Radiation Detector

Madalina Gabriela Tarzila
Technical University, Bucharest, Romania

1. Introduction

The Transition Radiation Detector (TRD) is one of the main detector components of the ALICE experiment at the Large Hadron Collider (LHC). It increases the tracking performance of the ALICE central barrel detectors and provides separation of electrons from the large background of pions.

Used in the Compressed Baryonic Matter (CBM) experiment, the TRD will provide the electron identification and – together with a Silicon Tracking System (STS) – the tracking of all charged particles. In order to fulfill the CBM requirements, small prototypes of the TRD based on multiwire proportional chambers (MWPC) with pad readout were developed and tested^[1].

The planned accelerator facility at GSI, FAIR will provide high intensity beams of protons and antiprotons, nuclei up to uranium as well as radioactive beams. The main goal for the study of nucleus–nucleus collisions is the exploration of the phase diagram of Quantum Chromo-Dynamics (QCD). Lattice QCD (LQCD) calculations predict that, at high energy densities, the quarks and gluons are not anymore confined in ordinary hadrons, but are in a phase called Quark–Gluon Plasma (QGP), a state of matter which was the substance of our Universe in the first microseconds after the Big Bang^[2].

TRD has to provide, in conjunction with the RICH detector and the ECAL, sufficient electron identification capability for the measurements of charmonium and of low-mass vector mesons. The required pion suppression is a factor of about 100 and the position resolution has to be of the order of 200–300 μm .

In order to fulfill these tasks, in the context of the high rates and high particle multiplicities in CBM, a careful optimization of the detector is required.

2. TRD

A TRD consists of two different main parts: a radiator, in which an electron creates the transition radiation, and a detection part consisting of a multiwire proportional chamber (MWPC) filled with a mixture of Xe and CO₂.

The MWPC subsumes a large area drift chamber with the drift direction perpendicular to the wire planes, and multiplication region. The electron identification is based on the measurement of energy loss^[3], dE/dx , by ionization and TR for electrons and dE/dx deposited by ionization for other charged particles. The MWPC technology also offers charged-particle tracking with a good position resolution due to a readout of the cathode which is subdivided into pads providing a high granularity.

2.1. Transition radiation and radiator:

Transition radiation (TR) a photon with an energy in X-ray range is produced by fast (*Lorentz factor* $\gamma > 1000$) charged particles at the crossing of boundaries between materials with different dielectric constants. In the momentum range from 1 to 10 GeV/c only electrons produce TR^[7]. The production probability is about 1% per boundary crossing, thus several hundred interfaces are used in practical TR detectors.

For the CBM TRD prototype the radiator is made of *ROHACELL* foam of 16 mm thickness.

2.2. Multiwire Proportional Chambers:

The TRD, proposed for the CBM experiment, consists of layers made of a dielectric radiator and a subsequent MWPC with pad readout. MWPCs are high-granularity fast detectors which allow track reconstruction of charged particles with good position resolution and the determination of their energy loss in the sensitive chamber volume. Furthermore, depending on the choice of gas,

these chambers are very convenient X-ray detectors which is important to measure the TR at the same time.

A basic MWPC consists of a plane of equally-spaced anode wires centered between two cathode planes. In principle, each wire acts as an independent proportional counter. If a positive potential is applied to the anode wires, the cathode planes being grounded, an electric field arises. In the region far away from the anode wires (~ 20 times the wire-diameter), the field lines are essentially parallel and the field density is almost constant. Close to the anode wires, the field shows an $1/r$ dependence similar to a single wire cylindrical proportional chamber. The wire radii, $20\ \mu\text{m}$ for the CBM prototype described below, are much smaller than the distance between the wires. This fact causes the electric field radial to the wire as seen in Fig.1 [4].

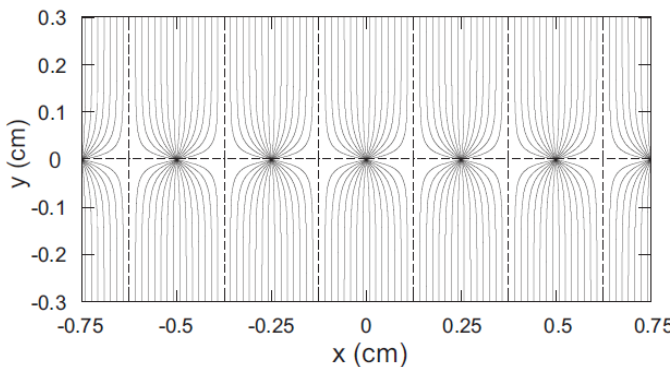


Fig 1. Schematic view of the electric field in an MWPC.

Far away from the anode wires, when electrons and ions are liberated in the constant field region, they drift along the field lines toward the nearest anode wire and opposing cathode. Near the high field region, the electrons are quickly accelerated and produce an avalanche. The electron avalanche is rapidly collected by the wires, the trailing positive ions move in opposite direction toward the cathode. In their motion, the ions induce image charges in all surrounding electrodes.

The cathode signal is read out, and the coordinate of the induced charge can be obtained by a subdivision of the cathode into readout pads perpendicular to the anode wires.

2.3. Gas mixture:

The filling gas for proportional counters has to meet different requirements: low working voltage, high gain, proportional

behavior, and high rate capability. For a minimum working voltage, noble gases are usually chosen due to the lowest electric field intensities necessary for avalanche formation.

Excited noble gas atoms formed in the avalanche deexcite giving rise to high-energy photons capable of ionizing the cathode and causing further avalanches. This problem can be minimized by the addition of a *quencher* such as CO_2 . The quencher molecules absorb the radiated photons and dissipate this energy through dissociation or elastic collisions.

The cheapest applicable noble gas is Ar because it is the largest noble gas contribution to the atmosphere. Nevertheless, the gas mixture in the TRD should be based on Xe because of its higher atomic number ($Z = 54$ in comparison to $Z = 18$ for Ar). The absorption coefficient for X-rays in the relevant energy region of the TRD is large enough only when using Xe [4].

In the TRD prototype, the gas mixture used is 85%Xe and 15% CO_2 .

3. Double-Sided TRD prototype

The double-sided TRD is a prototype based on a symmetric arrangement of two MWPCs with a double-sided central pad readout electrode. It was designed to resolve the small absorption probability for the transition radiation encountered by reducing the gas thickness of MWPCs in order to reach the required speed and to reduce space-charge effects caused by positive ions.

The detector is composed of two anode and two cathode frames, which are made of a 3mm printed circuit board (PCB) each. The two anode planes, placed at either side of the central pad readout electrode (pad plane), are made of gold plated tungsten wires with a diameter of $20\ \mu\text{m}$ and a wire pitch of $s = 2.5\text{mm}$. The anode-cathode gap h is 3mm; it has been optimized to provide appropriate charge sharing between adjacent pads. The entrance windows of $25\ \mu\text{m}$ aluminized polyimide foil serve simultaneously as gas barrier and cathodes[5].

Experimental setup:

The TRD is subjected to a series of laboratory tests:

- checking for tightness in order to obtain an O_2 concentration below 100 ppm;

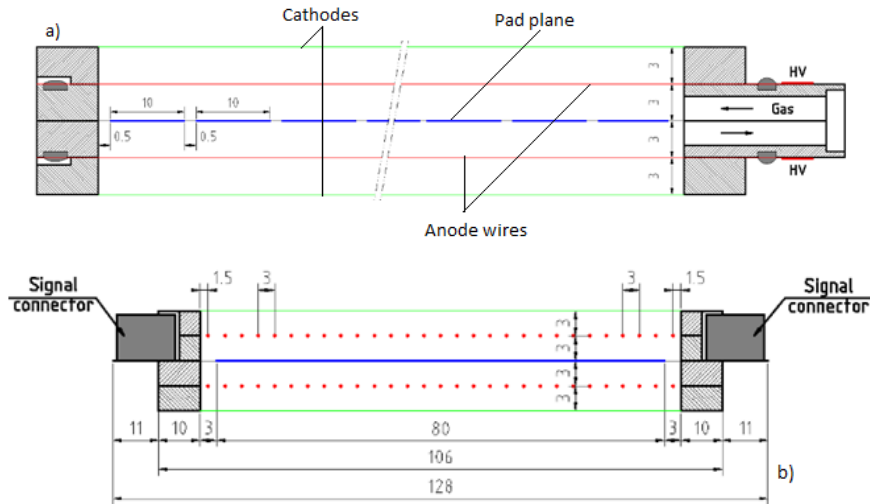


Fig 2 Schematic configuration of the TRD prototype: a) projection on a plane perpendicular to the detector surface and parallel to the wire direction and b) projection on a plane perpendicular to the detector surface and anode wire plane.

- high voltage endurance;
- energy resolution, measured using a ^{55}Fe X-ray source;
- position resolution, measured using a ^{238}Pu X-ray source;

For the position resolution the detector was tested using a ^{238}Pu X-ray source. The experimental setup is sketched in Fig. 3.

The measurements were performed at 1750V anode voltage using an Ar(70%)CO₂(30%) gas mixture. Custom built charge-sensitive preamplifier/shapers were used to process the detector signals which were digitized by a peak sensing ADC. The source was collimated onto the central pad.

Position Resolution

A charged particle traversing the detector creates a signal via gas ionization. The charge cluster can be reconstructed from the signal distribution on adjacent readout pads at the cathode pad plane. With this information, the position of the cluster can be determined

with better resolution than that obtained for a single pad. In order to achieve the best possible position resolution the induced charge distribution should be shared between typically two or three adjacent pads. The degree of charge sharing is given by the Pad Response Function (PRF), defined as the ratio of the charge deposited on a pad i (Q_i) to the total charge on three adjacent pads ($Q_{\text{tot}} = Q_{i-1} + Q_i + Q_{i+1}$) as a function of the position of the hit relative to the pad center x [1]. For each event, the central pad is determined as the pad with the maximum charge. The position of the hit can be reconstructed using one of the following formulas:

$$x = \frac{W}{2} \frac{\ln(Q_{i+1}/Q_{i-1})}{\ln(Q_{i+1}^2/Q_{i-1}Q_i)} \quad [4]$$

Or

$$x = \frac{1}{w_1 + w_2} \left[w_1 \left(-\frac{W}{2} + \frac{\sigma^2}{W} \ln \frac{Q_i}{Q_{i-1}} \right) + w_2 \left(\frac{W}{2} + \frac{\sigma^2}{W} \ln \frac{Q_{i+1}}{Q_i} \right) \right] \quad [5]$$

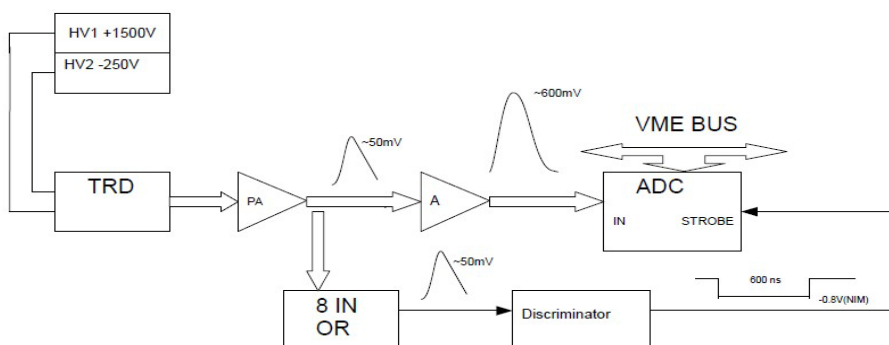


Fig 3 Experimental setup

where x denotes the distance of the hit from the center, and Q_i, Q_{i-1}, Q_{i+1} the charge on the center pad i and on the neighbouring pads on the left and on the right, and we choose :

$$w_1 = Q_{i-1}^2 \quad \text{and} \quad w_2 = Q_{i+1}^2.$$

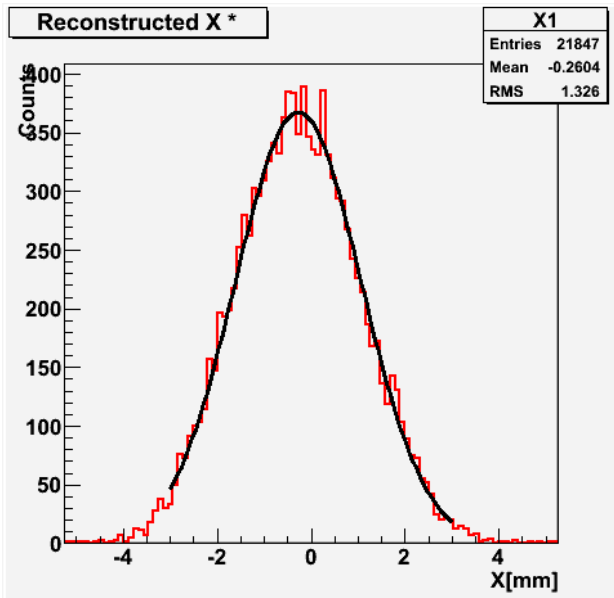


Fig 4.1

The results are presented in Fig.4.1 for the first formula [4] and in Fig.4.2 for the second one [6]. The scatter points are fitted with a Gaussian function to the mean of each channel in the interval $[-3,3]$. The standard deviation of the Gaussian^[5] obtained from fits were 1.34mm for [4] and 0.97mm for [6].

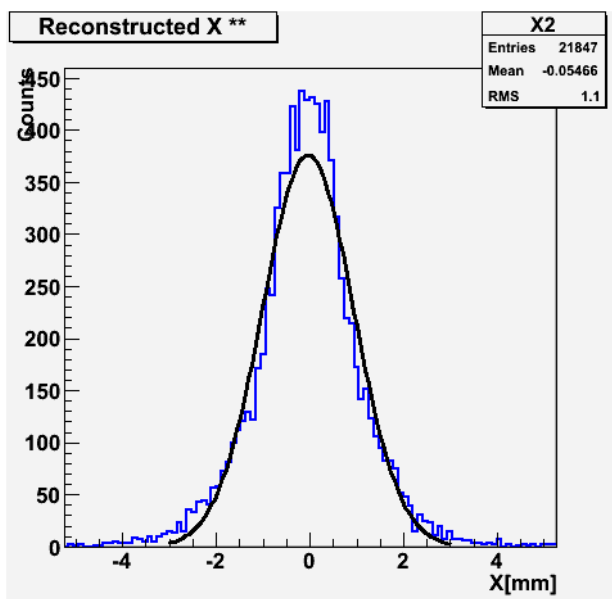
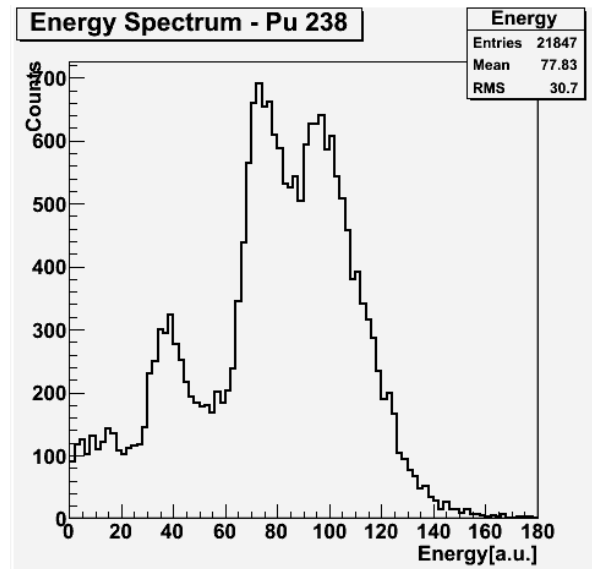


Fig 4.2

Next, the energy spectrum for a ^{238}Pu was obtained as a signal sum on all the readout pads.

Fig 4.3 Energy Spectrum for ^{238}Pu .

In conclusion, the double sided split pad prototype was designed, constructed and tested using radioactive X-ray sources. Preliminary results in term of energy and position resolution show a good performance. Detailed tests using e and π beam, will be done in the near future at PS-CERN.

4. References

- [1] .A. Andronic et. al., Nucl. Instr. Meth. Phys. Res. A 563 (2006), 349-354.
- [2] .M.Petris, M.Petrovici et al. High Counting rate transition radiation detector, Nuclear Instruments and Methods in Physics Research A 581 (2007);
[2] .FAIR, <http://www.gsi.de/fair/i/>; CBM, <http://www.gsi.de/fair/experiments/CBM/i/>.
- [3] .B. Dolgoshein, Nucl. Instrum. Meth. A326 (1993) 434.
- [4] .Melanie Klein-Bösing, Development of a Transition Radiation Detector and Reconstruction of Photon Conversions in the CBM Experiment, 2009, PhD thesis
- [5] .M. Petrovici et al., Nucl. Instrum. Meth. A579 (2007) 961.
- [6] .W. Blum and L. Rolandi, Particle Detection with Drift Chambers, Springer-Verlag, 1994.
- [7].ALICE TRD Technical Design Report, CERN/LHCC 2001-021, ALICE TRD 9, 3 October 2001.

Working principles of RPCs

Sebastian Toma

Technical University, Bucharest, Romania

1. Introduction & Brief History

The goal of the CBM Experiment (Compressed Baryonic Matter) is the investigation of highly compressed nuclear matter; matter in this form existing in neutron stars and in the core of supernova explosions. In an accelerator facility (such as FAIR – Facility for Antiproton and Ion Research), super-dense nuclear matter can be created in the reaction volume of relativistic heavy-ion collisions. The baryon density and the temperature of the fireball reached in such collisions depend on the beam energy, therefore, by varying the beam energy within certain limits, it is possible to produce different states and phases of strongly interacting matter, represented in figure 1.

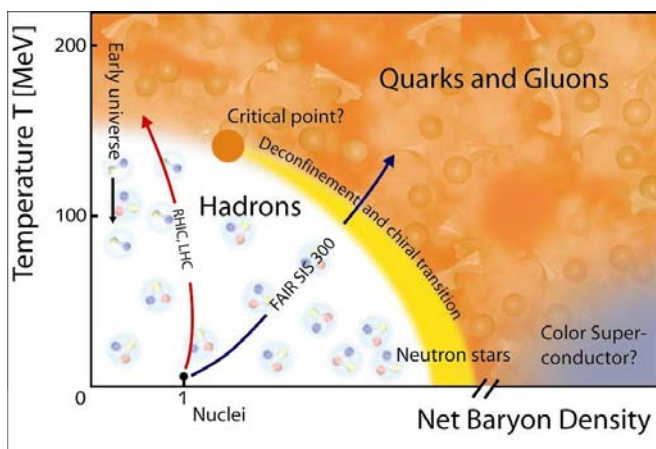


Fig 1

At low densities, the nucleons behave like a gas. By raising the temperature and the density, the nucleons are excited into "baryon resonances" which subsequently decay into pions and nucleons. This new mixture of nucleons, baryonic resonances and mesons is called hadronic matter (the white area from fig.1). At very high temperatures the hadrons 'melt' and their constituents, the quarks and gluons, form a deconfined phase of matter, called quark-gluon plasma. The phase transition

from hadronic matter to quark-gluon matter takes place at a temperature of about 170 MeV, meaning conditions similar to those of the early universe – the first few microseconds after the big bang.

Little is known about the critical density at which this transition occurs, yet the transition is predicted to change its character. The new FAIR facility permits the exploration of the this new field of the QCD phase diagram in the region of high baryon densities. In order to investigate the behaviour of nuclear matter in extreme conditions, the CBM Experiment aims to determine simultaneously various particles and so to determine particle multiplicities, phase-space distributions, collision centrality and the reaction plane.

Several types of particle detectors are to be used in the experiment, among which Time-Of-Flight (TOF) detectors – the Resistive Plate Counter (RPC) design - currently under development at NIPNE.

In the last three weeks I took part in the testing of a new type of glass proposed to be used in the Multigap Multistrip RPC, initially developed at NIPNE.

2. Physics and development of the RPC

TOF measurement is an important tool used in particle identification (PID) in relativistic and ultrarelativistic heavy-ion collisions.

Given the high velocities and large multiplicities in these collisions, the detectors are required to have a time resolution of well below 100ps. Standard scintillator-based instrumentation is expensive and implies complex electronics, whereas gaseous detectors have proven to be a viable alternative from both points of view. The typical design used for TOF

detectors is that of a PPC (parallel plate chamber). Historically, the first such counters were the Pestov Counters (1971)^[1].

Pestov counters work in the spark regime; they are operated at 12 bar with a highly quenching gas mixture. The gap of 0.1 mm is formed by a conductive electrode (normally a polished aluminum plate) and a semiconductive glass plate (schematically in figure 2). This special “Pestov glass” has a resistivity of about $5 \cdot 10^9 \Omega\text{cm}$. The streamer is followed by a spark which is quenched very quickly. The output signals are high; they can be plugged directly into double-threshold discriminators which guarantee a walk-free timing. Ninety centimeter long prototypes (with an area of 380 cm^2), developed at GSI, have reached time resolutions of about 60 ps with signals read out on both sides via individual anode strips; but building a Pestov detector has several technological difficulties such as the preparation of the electrodes, the technique of the 0.1 mm high spacers, the gas vessel holding 12 bar and the extreme requirements in cleanness during mounting and operation.

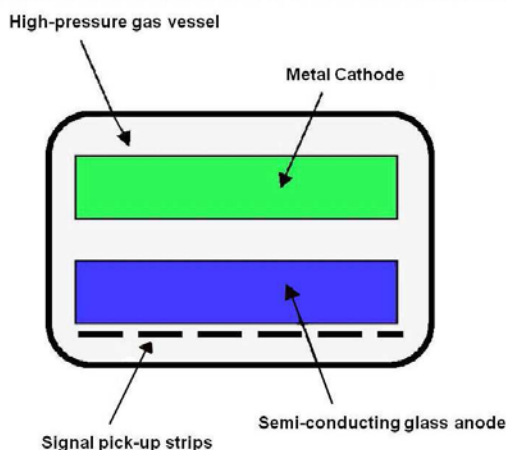


Fig 2

Also, the biggest difficulty is obtaining raw material of high quality and large sample size. An RPC is a parallel plate chamber with glass electrodes having a resistivity of the order of $10^{12} \Omega\text{cm}$ (therefore at least 100 times higher than that of Pestov glass). With a proper gas mixture the streamer development is suppressed and the discharge is limited to an

area around the primary avalanche causing high voltage drops only locally, so the remaining counter area is still sensitive to charged particles. The chamber operates in avalanche mode and requires fast amplification for its signals.

In its simplest configuration, the RPC detector is shown in figure 3 ^[2]. It consists of two electrodes made out of a resistive material (typically glass or bakelite) having bulk resistivity of $10^{10} - 10^{12} \Omega\text{cm}$ spaced by a few mm. The electrodes are connected to a high voltage power supply in order to create a uniform and intense electric field (about 5 kV/mm) in the gap between them. A thin layer of graphite is coated over the external surface of the electrodes to permit uniform application of the high voltage.

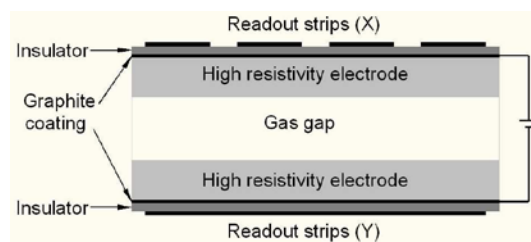


Fig 3

The electrodes are kept apart by means of small polycarbonate cylindrical spacers having a diameter of $\sim 0.1 \text{ mm}$ and a bulk resistivity greater than $10^{13} \Omega\text{cm}$. A gas mixture could consist of Argon, Isobutane and an electronegative gas like Freon (R134a). Argon acts as target for ionising particles while Isobutane, being an organic gas, helps to absorb the photons that result from recombination processes thus limiting the formation of secondary avalanches far from the primary ones. An electronegative gas may serve the purpose of limiting the amount of free charge in the gas. This type of gas mixture is particularly important when one wants to avoid the onset of streamers. The surface resistivity of the graphite coating is high enough to render it transparent to the electric pulses generated by the charge displacement in the gas gap. For this

reason electric signals can be induced on metallic strips capacitively coupled to the gap.

The strips are mounted on the external surface of the gap from which they are separated by a layer of mylar insulator. Two different sets of strips oriented in orthogonal directions may be arranged on both sides of the detector to obtain measurements in both planes. The strips behave like transmission lines with typical characteristic impedance of about 50Ω . High resistivity of the electrodes prevent high voltage supply from providing the electric charge that would be necessary to maintain the discharge between the electrodes. Therefore the electric field drops drastically in the region of the discharge causing it to extinguish. This behaviour can be understood by observing that the typical duration of the discharge is 10 ns while the time constant (τ) with which the electrodes are recharged is independent of the detector surface dimensions and is of the order of $\rho\epsilon$, where ρ and ϵ are the resistivity and dielectric constant of the glass. Assuming $\rho = 5 \cdot 10^{12} \Omega\text{cm}$ and $\epsilon = 4 \cdot \epsilon_0$ then $\tau \approx 1.8 \text{ s}$. The large difference between τ and the typical discharge time in the detector ensures that the electrodes behave like insulators during the discharge. Hence only a limited area (typically about 0.1 cm^2) of their surface suffers from a high voltage drop. This area stays inactive for a time interval of order τ . This represents the detector dead time in the region of the primary ionisation. Counting rate capability of an RPC is governed by these characteristic times. Glass RPCs can therefore handle counting rates of up to about $500\text{Hz}/\text{m}^2$ with a dead-time of less than 1%. Since typical bulk resistivity of bakelite is two orders of magnitude lower than that of glass, the rate capability of bakelite RPCs is proportionally higher. [1]

Research & development has resulted in multigap RPCs and consequently, at NIPNE, a new design – an improvement of the MRPC – that of a multistrip detector.

The principle behind the multigap design is to get many avalanches to act together: increase the gas gain (immediate production of a signal) while stopping the growth of avalanches. This is done by imposing barriers, as seen below, figure 4:

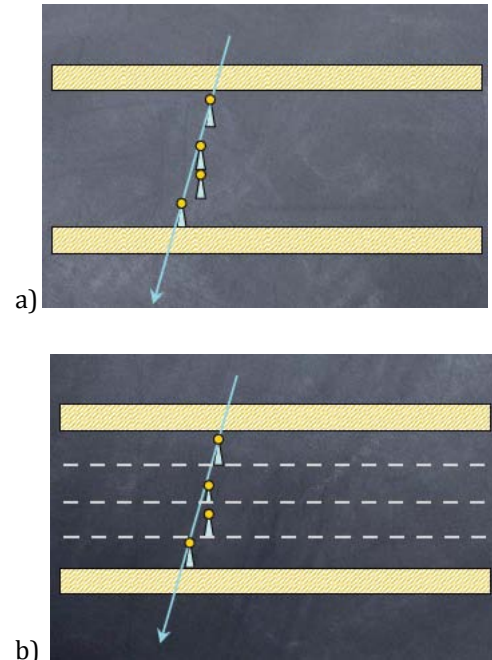


Fig 4

- a) normal avalanche development
b) charge formation after adding boundaries

The most prominent feature of this design is the inclusion of resistive, electrically floating electrodes that divide the gas volume into a number of individual gas gaps, without the need of any conductive electrodes. According to its inventors the steadystate requirement for a null total current on each of the dividing electrodes stabilizes their potential at a value that equalizes the currents flowing in and out by adjusting the gas gain in the neighboring gaps. Intermediate plates are *transparent* for avalanche signals; thus induced signals on external anode and cathode are *analogue sum* of avalanches in all gaps. The avalanches in different gaps have the same time development.

3. RPCs built and tested at NIPNE

As mentioned earlier, R&D conducted at NIPNE has resulted in a new and improved model for a gaseous counter – the multigap

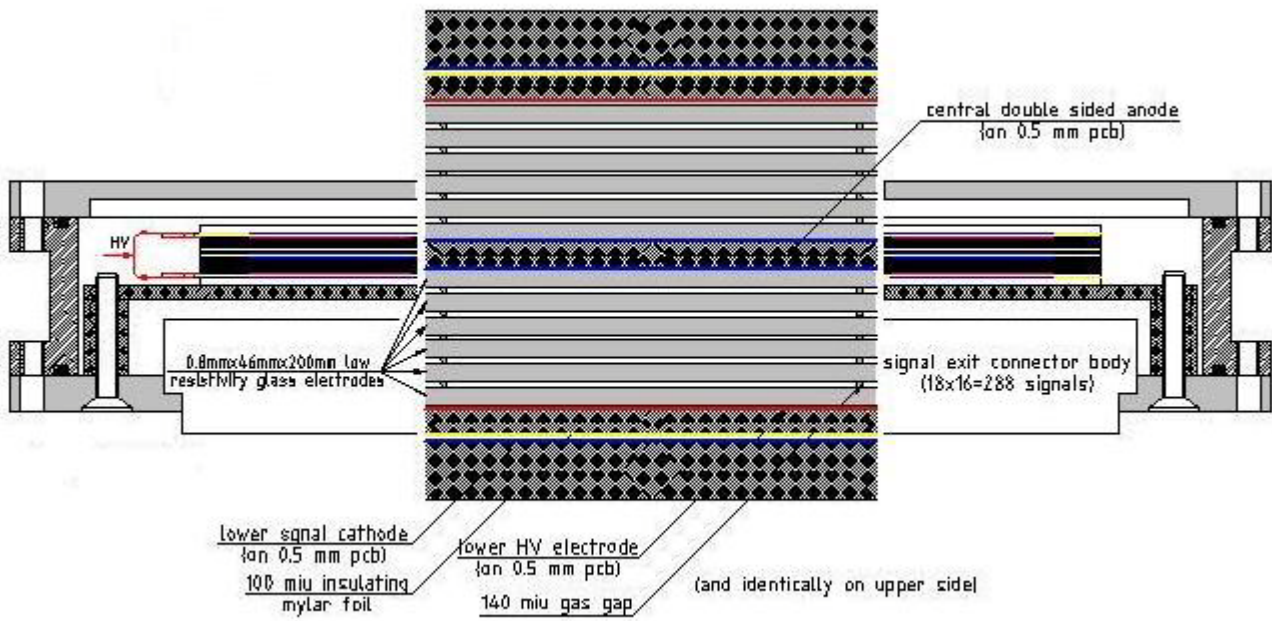


Fig 5

multistrip RPC.

Tests with ^{60}Co source and in-beam at GSI have indicated excellent time resolution (average of 80ps) and efficiency (96%)^{[3][4]}.

The most recent tests were aimed at verifying a new type of glass, used as the resistive plates; this new type of glass has a resistivity of $4 \times 10^{10} \Omega \text{cm}$. The experimental setup in this case was that of a single-strip counter. The final design is represented in figure 5.

The structure is the one used in the ALICE-TOF, having 10 gas gaps in two stacks of 5 each.

The high-voltage is applied only on the outer surfaces of each stack of glass, thus

making the inner part electrically floating, and easy to build. The readout and high voltage electrodes are made from a PCB of $\sim 500 \mu\text{m}$ thickness, without strip structure. As counting gas we use the standard mixture of 85% $\text{C}_2\text{F}_4\text{H}_2$; 10% SF_6 and 5% C_4H_{10} (isobutane) which is flushed at normal pressure. A schematic of how the signals are formed and collected is represented in figure 6.

However, the first trials have been unsuccessful, results indicating a spark regime inside the counter. One possible conclusion at this time is that the glass we were provided with has microimpurities -with very low resistivity - facilitating discharges.

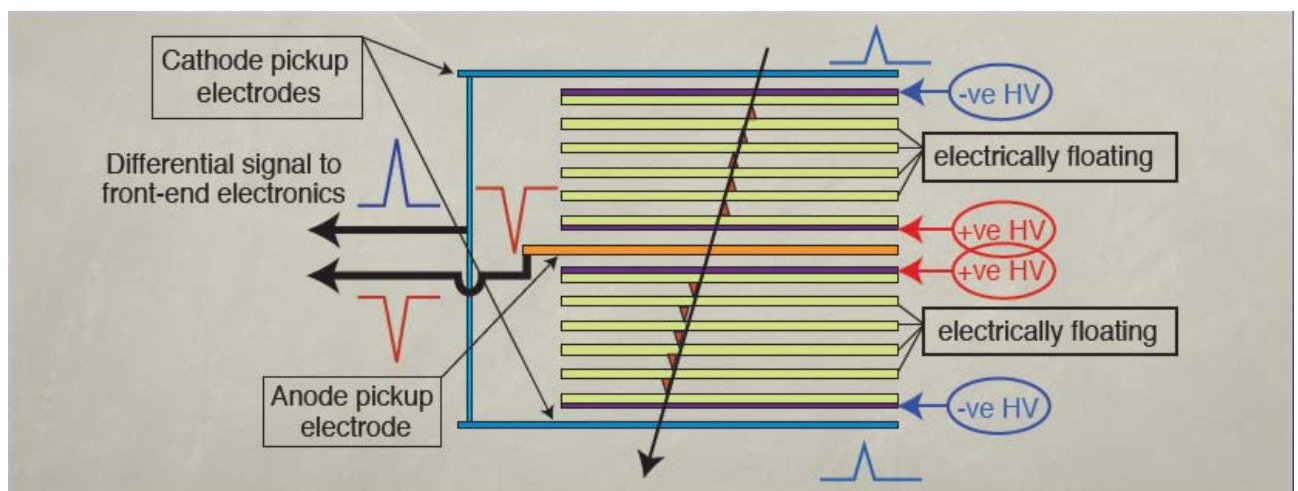


Fig 6

4. Conclusion

^{60}Co and in-beam tests show a high performance in terms of time and spatial resolution and efficiency. The present R&D activities are concentrated on testing low resistivity electrodes in order to conserve the above mentioned performances in high counting rate environment.

5. References

- [1] Satyanarayana Bheesette, 'Design and Characterisation Studies of Resistive Plate Chambers', PhD Thesis, Indian Institute of Technology Bombay, India
- [2] Christian Lippmann, 'Detector Physics of Resistive Plate Chambers', PhD Thesis, Johann Wolfgang Goethe-University
- [3] M. Petrovici, N. Herrmann, K.D. Hildenbrand, G. Augustinskib, M. Ciobanu, I. Cruceru, M. Duma, O. Hartmann, P. Koczon, T. Kress, M. Marquardt, D. Moisa, M. Petris, C. Schroeder, V. Simion, G. Stoicea, J. Weinert, 'Multistrip multigap symmetric RPC'
- [4] M. Petrovici, N. Herrmann, K.D. Hildenbrand, G. Augustinskib, M. Ciobanu, I. Cruceru, M. Duma, O. Hartmann, P. Koczon, T. Kress, M. Marquardt, D. Moisa, M. Petris, C. Schroeder, V. Simion, G. Stoicea, J. Weinert, 'A large-area glass-resistive plate chamber with multistrip readout'

The build-up of an RPC

Cristian Vlad

Technical University, Bucharest, Romania

1. Introduction

This report is a short summary of my three weeks at IFIN-HH DFH at Magurele. A bright experience that surely will be useful in my long waited career. In this period of time, we assembled a single cell multi-gap RPC (SSMGRPC) to test a new glass imported from China, with a resistivity of $4 \times 10^{10} \Omega \text{cm}$.

Also I will include a brief history, abstract –the basic principle of operation, types of RPCs and, the main purpose of this pages, the detailed process (step by step) of building the testing device (the RPC mentioned earlier) and what we have aimed in order for that glass to pass the test, and to replace the previous one.

2. Brief history

Resistive plate chambers (RPC) are fast gaseous detectors that provide a muon trigger system parallel with those of the Drift Tube Chambers (DTs) and Cathode Strip Chambers (CSCs)^[1].

RPCs were first introduced in 1981 ^[2] having a very practical design, making them free of damaging discharges and reaching a time resolution of the order of 1 ns, thus very attractive in High Energy and Astroparticle Physics.

The original RPCs were single-gap (fig. 1) counters operated in streamer mode. Soon after, the double-gap structure (fig 2.) ^[3] was introduced to improve the detection efficiency along with the avalanche mode of operation, which extends its counting rate capabilities. In 1996 a further improvement has been made resulting in the “multi-gap RPC”^[5](Fig. 3).

Innovations in detector construction and readout electronics have extended the timing resolution of RPCs for minimum ionizing particles (MIPs) to 50 ps ^[6], the rate capability to 10^5 Hz/mm^2 ^[7] and the position resolution for X-rays to 30 μm FWHM in digital readout mode ^[8].

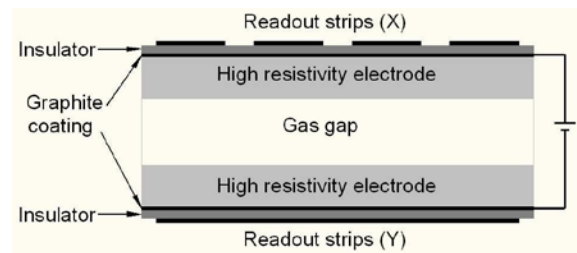


Fig 1 Constructional schematic of the original Resistive Plate Chamber

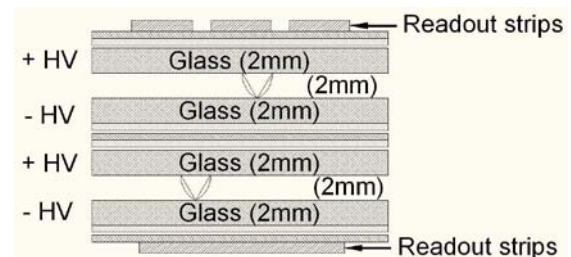


Fig 2 Schematic of a double gap Resistive Plate Chamber^[4]

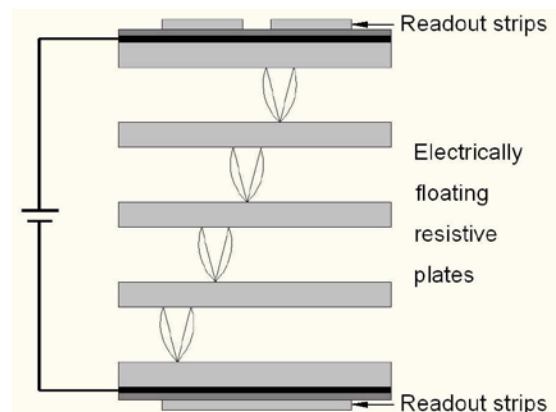


Fig 3 Schematic of a multi-gap Resistive Plate Chamber^[9]

Research and development at NIPNE has resulted in a novel concept of a multigap resistive plate chamber with multistrip readout electrodes^[10].

3. The Basic principle of operation^[11]

The task of a detector system in general is to identify and to measure the momenta and/or energies of different particles, which leave their trace in the detectors. The physical process upon which any gas detector is based, is ionization.

The RPC detector in its simplest configuration (fig. 1) : two planar electrodes

made out of a resistive material (glass or bakelite – in our case glass) having bulk resistivity of 10^{10} - 10^{12} Ω -cm are spaced by a few mm. The electrodes are connected to a high voltage power supply in order to create a uniform and intense electric field (about 5 kv/mm) in the gap between them. A thin layer of graphite is coated over the external surface of the electrodes to permit uniform application of high voltage. The electrodes are kept apart by means of small polycarbonate cylindrical spacers having a diameter of ~ 100 μm and a bulk resistivity greater than 10^{13} Ω -cm. A gas mixture could consist of Argon, Iso-butane and an electronegative gas like Freon (R134a).

4. Types of RPCs

Due to a large variety of requirements, physicists have come up with many designs of RPCs. They came up with a rich variety of combinations of resistive and/or metallic electrodes, signal-transparent semi-conductive electrode coats, highly isolating layers between the electrodes and signal pick-up panels. Here are a brief description of RPC designs^[10]

4.1. Single gap RPC (fig. 1)

The original RPC design, bakelite resistive electrodes delimiting a single gas gap. However, how time passed, a number of improvements have taken place in the chamber. Glass electrodes have replaced the bakelite due to a mechanical rigidity and better surface quality.

4.2. Double gap RPC (fig. 2)

Double gap designs having a larger number of elements (such as gas gaps and pickup electrodes), allow for more varied chamber structures than the single gap ones.

Alternately, double gap RPCs are also made of two independent gas gaps with a common pick-up panel sandwiched in the middle (symmetric RPC)^[12].

4.3. Multi-gap RPC (fig. 3)

While the construction of the single gap RPCs is simple and well suited for most applications, there are some inherent drawbacks in its design.

In order to alleviate the problems, a novel construction method, denominated multi-gap RPC was introduced, being specially suited for the construction of counters with more than a single gas gap.

The most prominent feature of this design is the inclusion of resistive, electrically floating electrodes that divide the gas volume into a number of individual gas gaps, without the need of any conductive electrodes.

Other designs that have been used are Hybrid RPCs, Micro RPCs, Multi-strip Multi-gap RPCs (MSMGRPC), SSMGRPCs – presented in details in the next chapter, because this was our experimental device.

5. The core of the article

Now that we have a bit of knowledge about RPCs from the short introduction above, I can move on with the main part.

Testing the new doped glass imported from China (fig. 4).



Fig 4 Low resistivity glass – China Glass

This glass was embedded into a SSMGRPC, with 6 glass plates, and 5 gas gaps.

5.1. The construction of the experimental device

As mentioned earlier the device used to test this new glass was a SSMGRPC. The cathodes, and the HV electrode, were made of copper-clad plate pcbs (printed circuit boards) about 1.5 mm thick, while the anode was double-sided copper-clad also on a 0.5 mm pcb

On a 3 mm stesalit plate we mount the lower signal cathode above which we put a 100 μm insulating mylar foil, and on top of it a lower HV electrode. After this is done, in direct contact with the HV electrode, we put the first glass plate. On six pivotal nylon screws - three on the left, and three on the right - we coil the fishing line (fig. 5), making so the first gap. We next come with the second glass plate over which again the fishing line. We repeat this sequence of glass and fishing line like in the end to have 5 gaps (6 glass sheets).



Fig 5 Fishing line coiled on a pivotal screw

The thickness of the glass is 0.8 mm.

On top of the structure described above, we mounted the central electrode - double sided anode - also in direct contact with the last lower glass and the first upper one, which we mount on the anode. We repeat all the other procedures in retrograde order, namely, glass, nylon, glass - forming 5 gaps - then the HV electrode, afterward the mylar foil, and on top de upper cathode. After this is done, we mount the brackets to hold the whole assembly in place (fig. 6).

We then connect the signals, we sum the two cathodes (the first signal), and the anode the second one. We make the HV connections

binding the 2 HV electrodes, that we have mounted on the RPC, with a point of ingathering brought by the external card.

When all of these is done, we put the whole thing in an insulated metal box so we connect the gas mixture to circulate through it.

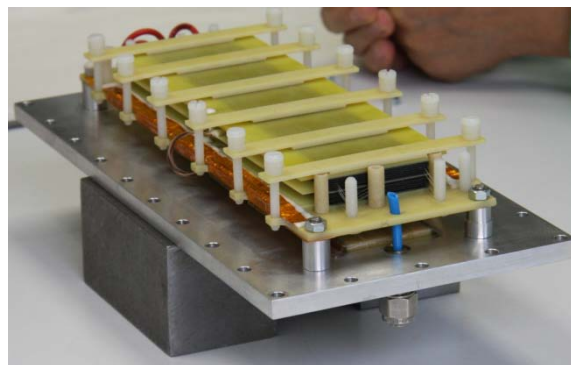


Fig 6 Our SSMGRPC

5.2. Concept - reality

Before the beginning the production of the pieces whom combined build-up the device, of course it was needed a graphic design. All the components, the anode, the cathode, HV electrode, were graphic made on PC, with the help of Qcad. Even the entire assembly (fig. 7) was done, 1:1 scale, but it was only made 2D.

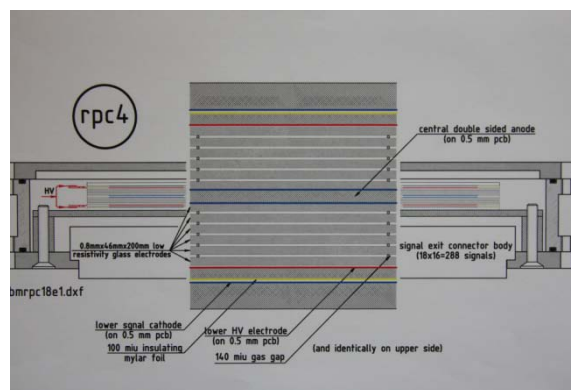


Fig 7 The assembly - graphic made - and a pop-upped section

5.3. The gas mixture

Here we have worked with a new installed device, that mix-up our three gases.

The mixture is composed of isobutan, freon 134, and sulphur hexafluoride, all in good proportions.

In our case, we used the following:

- Isobutan - 5%

- Freon 134 – 85%
- Sulphur hexafluoride – 10%

After few numerical calculations we obtained for every gas apart, the flow for a total debit quantity of 30 mln/min. For isobutan – 2.3979 mln/min, for freon – 23.1615 mln/min, and for sulphur hexafluoride – 4.509.

We then connect the whole device to HV – 5000 V, and we look at the signal to see if there are good or not.

But, after we let the gas flow, we must wait one or two hours so that the volume of the gas that passed through our RPC to be 7 times bigger than our metal box volume. That is made so in order for the signal to be correct.

Very important aspects that we must take in consideration are, the aging of the glass, the detection efficiency, and the timing resolution, that must be well below 100 ps.

6. Conclusion

The detection system based on RPC has proven itself due to outstanding properties:

- Timing resolution - well below 80-100 ps – by special means of construction, it can go at ~30 ps.
- High efficiency -> can reach 100%
- Simple design with common materials – pcb, glass, fishing pole
- Simple operation with common detection gases
- Various designs - can be built to meet the requirements of the experiment

It is worthy of note that the investigations currently performed for RPC with high granularity for CBM experiment at high beam intensities.

7. References

- [1]. <http://cms.web.cern.ch/cms/Detector/Muons/PlateChambers.html>
- [2]. Santonico and R. Cardarelli, "Development of Resistive Plate Counters", *Nucl. Instr. Meth.*, vol. 187, pp. 377-380, 1981.
- [3]. R. Cardarelli and R. Santonico, A. di Biagio and A. Lucci, "Progress in resistive plate counters", *Nucl. Instr. Meth.*, vol. A263, pp. 20-25, 1988.
- [4]. K.Abe *et al.*, *Scientifica Acta* **13**, (1998), 281

- [5]. E. Cerron Zeballos, I. Crotty, D. Hatzifotiadou, J. Lamas-Valverde, S. Neupane, M. C. S. Williams, A. Zichichi, "A new type of resistive plate chamber: the multigap RPC", *Nucl. Instr. Meth.*, vol. A374, pp. 132-135, 1996.
- [6]. P. Fonte, R. Ferreira-Marques, J. Pinhão, N. Carolino, A. Policarpo, "High-resolution RPCs for large TOF systems", *Nucl. Instr. Meth.*, vol. A449, pp. 295, 2000.
- [7]. P. Fonte, N. Carolino, L. Costa, Rui Ferreira-Marques, S. Mendiratta, V. Peskov, A. Policarpo, "A spark-protected high-rate detector", *Nucl. Instr. Meth.*, vol. A431, pp. 154-159, 1999.
- [8]. V. Peskov and P. Fonte, "Gain, Rate and Position Resolution Limits of Micropattern Gaseous Detectors", presented at the PSD99-5th International Conference on Position-Sensitive Detectors, London, England, 1999.
- [9]. E.C.Zeballos *et al.*, *NIMA* **374**, (1996), 132
- [10]. M. Petrovici, N. Herrmann, K.D. Hildenbrand, G. Augustinskib, M. Ciobanu, I. Cruceru, M. Duma, O. Hartmann, P. Koczon, T. Kress, M. Marquardt, D. Moisa, M. Petris, C. Schroeder, V. Simion, G. Stoicea, J. Weinert, 'Multistrip multigap symmetric RPC', *Nucl. Instr. And Math.* A487(2002) 337.
- [11]. P.Fonte, *IEEE Trans. on Nucl. Sci.* 49 (2002), 881.
- [12]. CMS Collaboration, CERN/LHCC 97-32, (1997).

Other treasuries:

- 1) http://ppd.fnal.gov/experiments/e907/TOF/Alice_RPC_Design.pdf.
- 2) Satyanarayana Bheesette, "Design and Characterisation Studies of Resistive Plate Chambers", *Department of Physics Indian Inst. of tech. Bombay*, INDIA, 2009.
- 3) Christian Lippmann "Detector Physics of Resistive Plate Chambers", Frankfurt am Main, 2003.

MBS (Multi-Branch System)

Ioana Petrescu, Alexandru-Octavian Stanculescu
Technical University, Bucharest, Romania

1. Introduction

MBS stands for Multi-Branch System and it is a software environment developed at GSI for data acquisition purposes. The MBS data acquisition system runs under an UNIX based distribution, Lynx OS, and is based on multiple single branch systems (based on a single-crate CAMAC or VME system) that are interconnected using multiple intelligent controllers. The data connection between the crate controllers in the multi-branch system can either be memory mapped or transfer oriented.

This system is computer independent, a workstation could be needed only for on-line analysis.

The MBS is controlled using terminals through a command interface; the commands used to interact with the system are usually composed of three keywords followed by arguments and qualifiers.

2. Software

MBS is controlled using a command-line interface. Each command is composed of up to three keywords followed by arguments. A set of commands that are used to serve the same purpose or that are used together to perform a task can be stored in text files and then executed as a batch when needed.

Examples:

```
SET VERBOSE EVENT
START TASK <name>
SHOW COMMAND
```

The MBS Environment is composed of commands that can either be started from the shell or run in background.

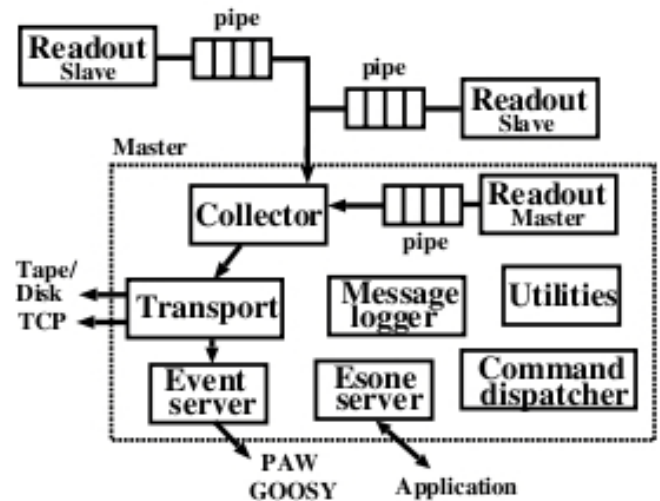


Fig 1 MBS Environment

3. Hardware

MBS can be used either as a single-crate or a single-branch system. Moreover, multiple single-branch systems can be connected in order to form a multi-branch system. MBS requires that every crate is equipped with a crate controller both intelligent or non-intelligent. The supported crates are CAMAC, VME and FASTBUS, each with the corresponding software prerequisites.

One of the controllers will act as the branch master therefore it must have read/write access^[1].

3.1. CAMAC

CAMAC stands for Computer Automated Measurement and Control and it is a Data acquisition and control standard bus that allows data exchange between modules that are plugged into crates (up to 24 in one crate). The communication and data handling is done using a crate controller which also facilitates communication with a PC or a VME-CAMAC interface^[2].

Each CAMAC module can be plugged in a crate which has 25 slots (STATIONS), numbered from 1 to 25. The last two STATIONS are

reserved for the crate controller which is responsible with data handling, inter-module communication and interfacing the CAMAC crate with a PC or other acquisition systems. The way the controller communicates with the modules is by issuing commands via the buses. The necessary power for the modules, the address N lines, control bus and data bus are provided by the DATAWAY which also includes data transfer lines, strobe signal lines, addressing lines and control lines.

A typical CAMAC command includes the NAF values (N – STATION NUMBER, A – SUBADDRESS and F – FUNCTION code). If the command is valid then the modules generates an X reply in order to notify the controller that the command was accepted and is going to be processed. For data transfer the CAMAC controller uses the READ (R) and WRITE (W) bus lines. Other lines are the LOOK-AT-ME (L), DATAWAY BUSY (B), RESPONSE (Q) which are used to generate status information and other control lines like INITIALIZE (Z), INHIBIT (I) and CLEAR (C).

The standard and mandatory power supply lines for the CAMAC system are +/-24V and +/-6V but other supplies could be needed in order to maintain compatibility with other modules like NIM.

3.1.1. CAMAC addressing methods

The STATION NUMBER N is a decimal representation from left to right of the position of a module and is used to address the specified module.

The SUBADDRESS (A8, A4, A2, A1) uses 4 bus lines in order to call a desired section of a module, therefore a total number of 16 subaddresses, numbered from 0 to 15 can be addressed using the 4 bit coded signal.

After addressing the station and it's subaddress a function must be sent in order to assign a task to the module. Thus, the 5 FUNCTION bus lines are used to send up to 32 possible functions to the module.

In order to initiate operations or transfer information between the units two special lines are used called STROBE lines. The signals sent via these lines are the STROBE SIGNALS (S1 and S2), both being generated by the controller during each DATAWAY command operation. The first STROBE SIGNAL (S1) is used in read or write operations and the second one (S2) is used to alter the state of the DATAWAY signals (e.g. clearing a register).

3.1.2. Data transfer

CAMAC systems are able to transfer up to 24 bits of data in parallel between the controller and an addressed module over independent lines (read and write).

The write lines (W1-W24) are used for write operations and the read lines (R1-R24) are used for read operations. Both signals reach a steady state before S1 and are maintained for the whole duration of the DATAWAY operation unless modified by S2.

The busy (B) signal is used to specify that an operation is in progress over the DATAWAY and whenever this signal is present all LOOK-AT-ME (L) signals are gated off the DATAWAY.

The X signal (COMMAND ACCEPTED) is used every time an addressed module recognizes a command received on the DATAWAY and it generates an X signal.

The RESPONSE line (Q) is used for status information during the execution of a task, thus keeping the crate controller informed about the state of the currently executed command [3].

3.2. VME

The VME(Versa Module Europa) is a computer bus standard originally developed for the Motorola 68000 line of CPUs, but later widely used for many applications and standardized^[4].

Three main types of cards reside on the VME bus are: the controller which supervises the bus activity, the Master that reads/writes data from/to a Slave board and the Slave interface that allows data to be accessed via a Read/Write from a Master^[5].

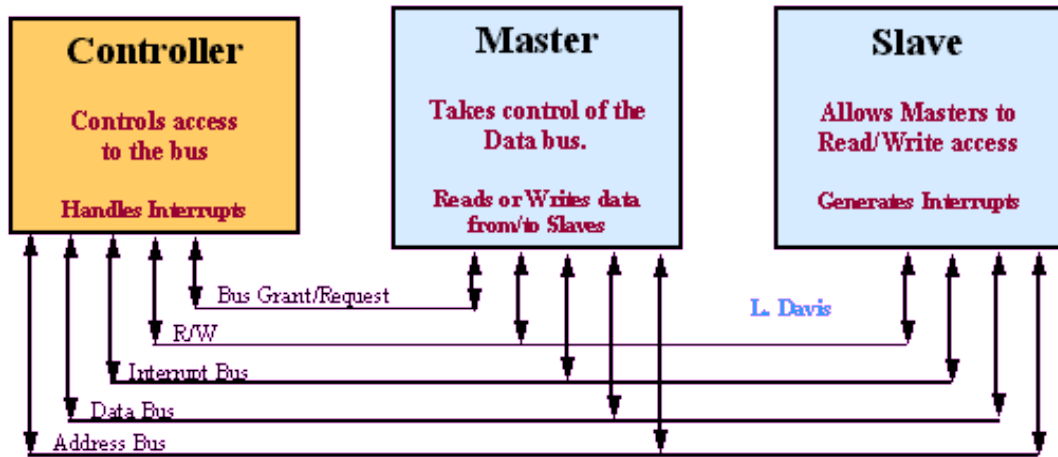


Fig 2 VME bus main types of cards

Since multiple Masters can reside on the bus, it is a Multiprocessing bus therefore it can take up to 21 Masters.

The VME bus is asynchronous meaning that there is no central synchronization clock, instead it uses a handshaking protocol [6].

“bus grants” the access, the Master drives Address and data bus to perform a data transfer to a Slave board.

Any number of Masters may reside on the VME, but only one may control the bus at any one time.

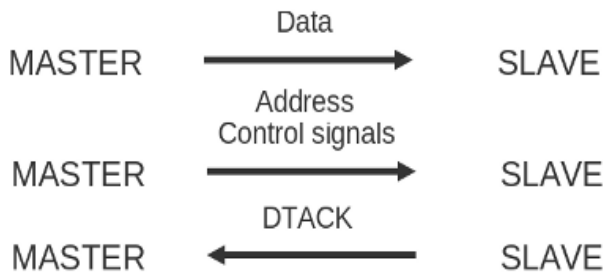


Fig 3 Handshaking protocol diagram

3.2.1. The Controller

It controls access to the bus: when receiving a “Bus Request” signal from a Master, it will “Bus Grant” that Master access to the bus.

It also handles interrupts on the bus : when receiving one on one of the lines, it will process the interrupt by accessing the interrupting card and acknowledge the interrupt.

Only one controller may reside on the VME bus.

3.2.2. The Master

It reads and writes data to or from a Slave board and it “bus requests” access to the VME from the controller. Once the controller

3.2.3. The Slave

It monitors the Address and Data bus for reads or writes sent to it. When a correctly decoded Address is received, it will either receive information for a write or output information onto the Data bus in case of a read. The Master continues to control the Data bus during either interface.

May also generate interrupts over any line[5].

There are 2 main types of data transfers on the bus: single cycle that consists of a Master performing an Address cycle followed by a single data transfer cycle (duration 1 μs) and it is controlled by the CPU and block transfer (BLT) that consists of a Master performing a single Address cycle followed by up to 256 data cycles and it is CPU independent.

For 256 bytes only one bus request cycle is required and only one Address cycle.

3.2.4. VME data width

During the start of a transfer, the Master will set the data transfer bus width using the two data strobes, Address bit 01 and 02, and LWORD.

The condition of these lines at the start of a data transfer informs the Slave of the incoming data bus width. The VME Address bus width used by the Master is determined by the setting of the Address modifier codes [5].

3.2.5. Arbitration

Before a master can transfer data it has to request the bus, by asserting one of the four bus request lines (BR). The arbiter knows if the bus is busy or idle. Once it is idle it asserts one of the four Bus Grant out Lines (BGOUT). If a master detects a 1 on the BGIN line corresponding to its BR it claims the bus.

If two masters use the same bus request level the one closer to slot 1 inherently has a higher priority.

Modern masters support “fair arbitration”, meaning they delay their bus request if other masters are requesting the bus at the same level.

With single master, when system boots, he master asks for the bus, gets it and keeps it. The VME provides 4 separate bus request levels. Arbitration is done by the System Controller and can be set up in: priority mode, round robin mode or single level mode.

3.2.6. Addressing

The VME bus provides a large variety of address spaces and data widths. It makes no distinction between IO space and memory space and it uses a 6 bit address modifier code to distinguish between three address spaces(16 bit, 24 bit, 32bit).

The VME bus backplane has 31 address lines. A slave is selected by two criteria : address and address modifier (the number of valid address bits, the access mode, the transfer type). Typically slaves respond to only one address width but may allow both single cycles and block transfers.

3.2.7. Interrupts

The VME bus provides 7 interrupt levels to prioritize interrupts. Each interrupter can use any level. For each level there must be only one interrupt handler. The interrupt handler uses a special type of single cycle to obtain a 8 bit vector from the interrupter. This vector must be unique and identifies the source of the interrupt.

There are two types of interrupters: ROAK(the IACK cycle clears the interrupt) and RORA(an additional register access clears the interrupt). If two interrupters are active at the same time and on the same level the one closer to slot 1 will be serviced first[6].

4. Local setup

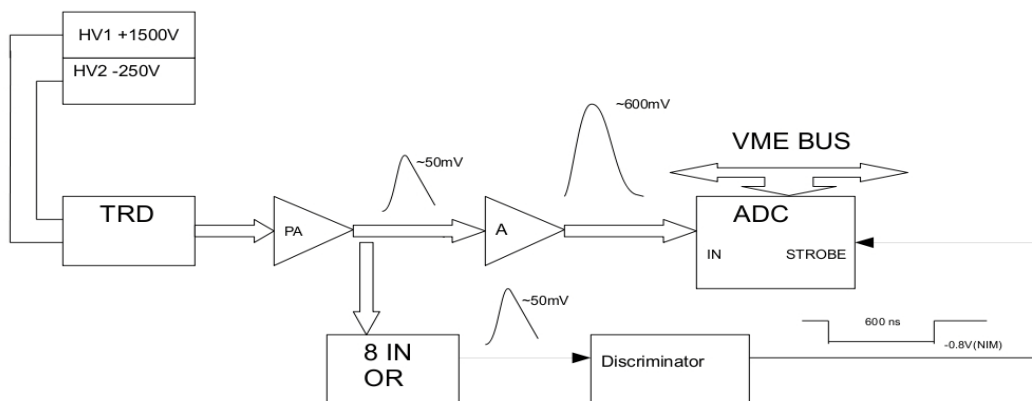


Fig 4 Block schema of local setup

Our initial local setup was based on CAMAC modules and the CAMDA software environment for data acquisition. Like MBS, CAMDA is a software developed by Herbert Stelzer at GSI, Darmstadt in Germany in order to facilitate the interaction of a PC with a CAMAC crate.

CAMDA runs under Microsoft Windows operating systems and was mainly written in Fortran with some parts written in Assembler and in C. It has a menu-driven graphical user interface and it features an online editable list (CAMAC-List) that contains all the CAMAC modules that can be accessed from CAMDA, their corresponding NAF commands and other definitions. CAMDA also has the feature of replaying (simulating) an acquisition from a local file where it has been previously recorded.

Later, we switched from CAMDA to MBS as for it uses VME modules and at this time it is more powerful and flexible than the CAMDA-CAMAC solution. At the beginning we encountered some problems regarding the MBS because it wasn't recognizing the new VME modules and had no function definitions for these modules due to the fact that it was previously setup to work with CAMAC modules. After solving the problem the system started to work almost at the desired parameters.

In order to justify the switch from CAMDA to MBS we will describe below, by comparison, a list of advantages that MBS has over CAMDA:

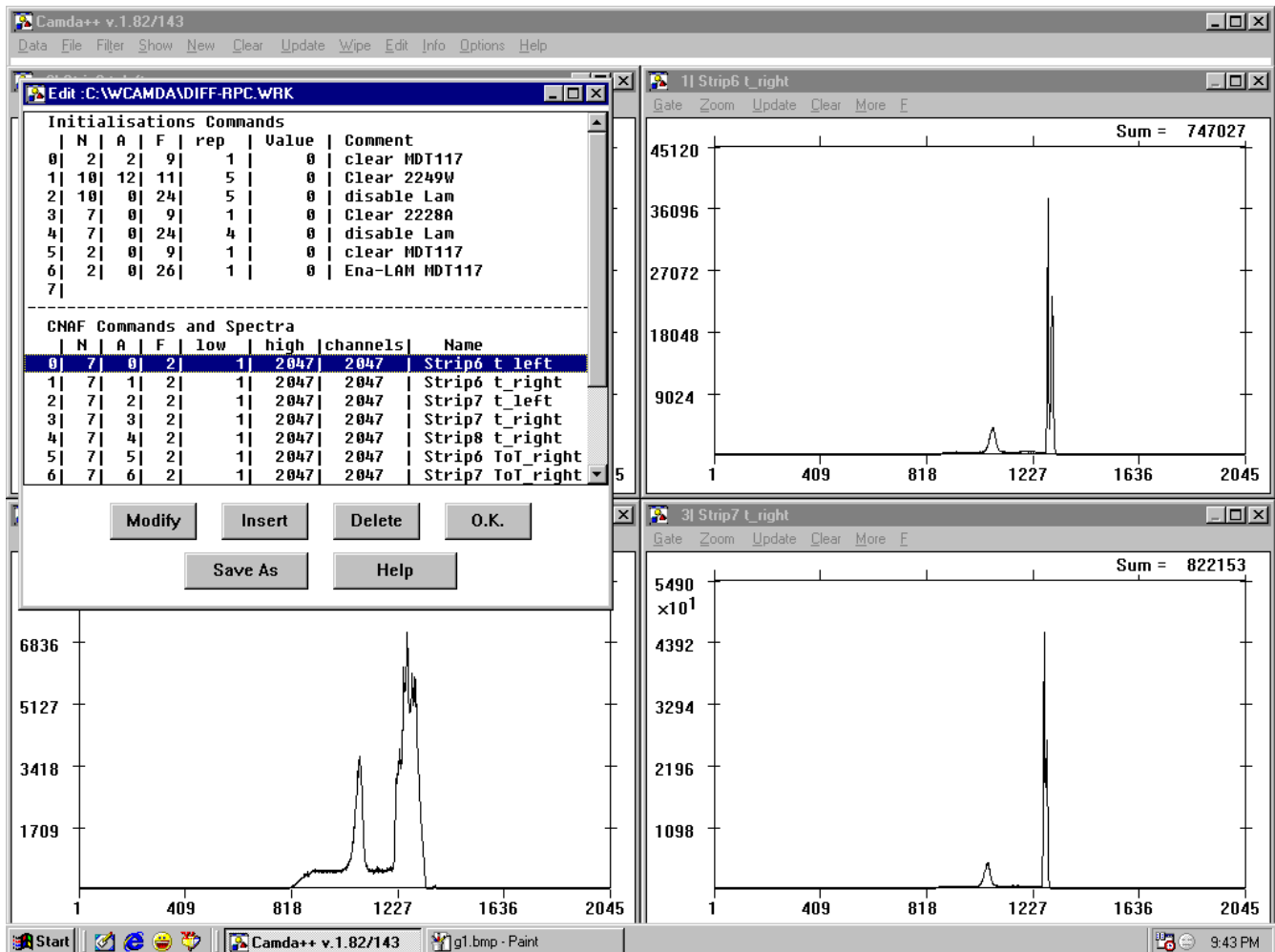
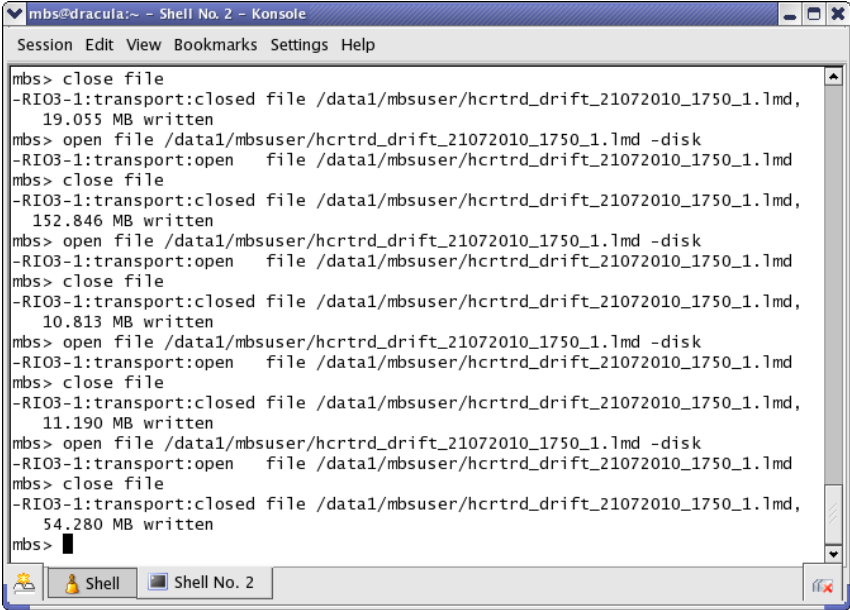


Fig 6 CAMDA GUI

MBS	CAMDA
<p>Runs on UNIX based operating system (LynxOS) therefore it provides a multi-user access to the system at the same time which is a great advantage for large experiments with many users involved and lots of data needed to be analyzed</p>	<p>Runs on Windows operating system and it only has single-user access possibilities, but it is good enough for small experiments and tests.</p>
<p>Communicates with VME modules which are newer and more powerful than the old CAMAC modules but it can also address CAMAC ones</p>	<p>Communicates only with CAMAC modules</p>
<p>Command based interface: it uses a shell and commands are needed to control and setup the system; even if it is harder to use for beginners it is more powerful, more flexible and it can be remotely controlled by multiple users</p>	<p>Uses a GUI but it's limited and can not be remotely controlled</p>



```

mbs@dracula:~ - Shell No. 2 - Konsole
Session Edit View Bookmarks Settings Help

mbs> close file
-RI03-1:transport:closed file /data1/mbsuser/hcrtrd_drift_21072010_1750_1.1md,
19.055 MB written
mbs> open file /data1/mbsuser/hcrtrd_drift_21072010_1750_1.1md -disk
-RI03-1:transport:open file /data1/mbsuser/hcrtrd_drift_21072010_1750_1.1md
mbs> close file
-RI03-1:transport:closed file /data1/mbsuser/hcrtrd_drift_21072010_1750_1.1md,
152.846 MB written
mbs> open file /data1/mbsuser/hcrtrd_drift_21072010_1750_1.1md -disk
-RI03-1:transport:open file /data1/mbsuser/hcrtrd_drift_21072010_1750_1.1md
mbs> close file
-RI03-1:transport:closed file /data1/mbsuser/hcrtrd_drift_21072010_1750_1.1md,
10.813 MB written
mbs> open file /data1/mbsuser/hcrtrd_drift_21072010_1750_1.1md -disk
-RI03-1:transport:open file /data1/mbsuser/hcrtrd_drift_21072010_1750_1.1md
mbs> close file
-RI03-1:transport:closed file /data1/mbsuser/hcrtrd_drift_21072010_1750_1.1md,
11.190 MB written
mbs> open file /data1/mbsuser/hcrtrd_drift_21072010_1750_1.1md -disk
-RI03-1:transport:open file /data1/mbsuser/hcrtrd_drift_21072010_1750_1.1md
mbs> close file
-RI03-1:transport:closed file /data1/mbsuser/hcrtrd_drift_21072010_1750_1.1md,
54.280 MB written
mbs>

```

Fig 7 MBS Shel

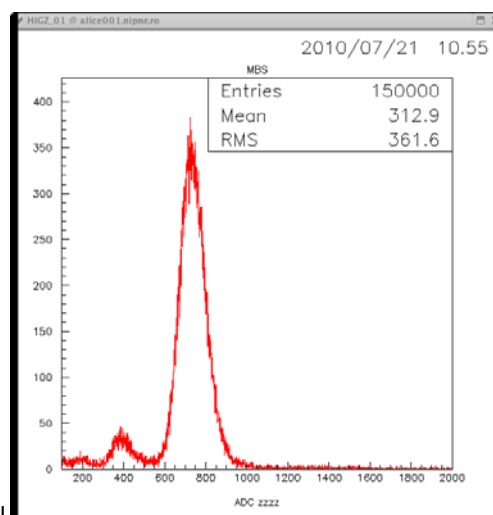


Fig 8 Spectrum obtained via MBS

In conclusion MBS is a software environment, developed at GSI, that provides the user with commands that are used to control the data acquisition process of various hardware configurations. The advantages of the MBS environment is that it can control different types of crates such as CAMAC, VME or FASTBUS and their corresponding modules and facilitates communication between these types of hardware.

5. References

- [1]. <http://www-win.gsi.de/daq/document.htm>
- [2]. [http://en.wikipedia.org/wiki/Computer Automated Measurement and Control](http://en.wikipedia.org/wiki/Computer_Automated_Measurement_and_Control)
- [3]. <http://www-esd.fnal.gov/esd/catalog/intro/introcam.htm>
- [4]. <http://en.wikipedia.org/wiki/VMEbus>
- [5]. [http://www.interfacebus.com/Design Connector VME.html](http://www.interfacebus.com/Design_Connector_VME.html)
- [6]. IEEE 1014-1987 standard specification
www.vita.com/vmefaq
www.hitex.com/automation/FAQ/vmefaq

ALICE TRD Reconstruction and Visualization

Mihai-Marian Puscas

Technical University, Bucharest, Romania

1. Introduction

ALICE is a general-purpose heavy-ion experiment designed to study the physics of strongly interacting matter and the quark-gluon plasma in nucleus-nucleus collisions at the LHC. [2]

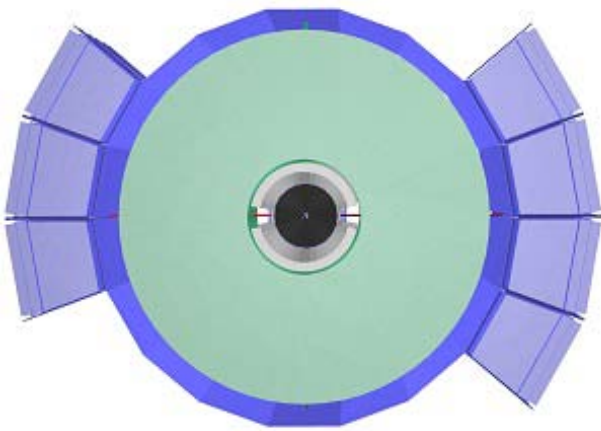


Fig. 1 TRD Supermodule

2. Transition Radiation Detector (TRD)

Transition Radiation Detector (TRD) is a main detector system of ALICE located in between the Time Projection Chamber (TPC) detector and Time of Flight (TOF). The main purpose of the **TRD** is to provide electron identification and tracking in the momentum range above 1 GeV/c. Therefore it has to be assured that a sufficient pion suppression can be achieved, even in the high multiplicity environment expected in the ALICE experiment. Additionally, a high tracking efficiency and good momentum resolution for particles in the momentum range of interest is required. There are currently 7 active TRD supermodules out of a planned 18^[1].

Detector requirements:

Momentum resolution	5.00% (for $p = 5\text{GeV}/c$)
Tracking efficiency	(for $p > 5\text{GeV}/c$)
Pion-rejection factor	100 (for 90% e-efficiency and $p \geq 3\text{GeV}/c$)

3. Reconstruction Framework

Event Reconstruction is the process of interpreting the electronic signals produced by the detectors to determine the particle's momentum, type, charge, decay vertex.

Digit: This is a digitized signal (ADC count) obtained by a sensitive pad of a detector at a certain time.

Cluster: This is a set of adjacent (in space and/or in time) digits that were presumably generated by the same particle crossing the sensitive element of a detector.

Reconstructed space point: This is the estimation of the position where a particle crossed the sensitive element of a detector (often, this is done by calculating the center of gravity of the 'cluster').

Reconstructed track: This is a set of five parameters (such as the curvature and the angles with respect to the coordinate axes) of the particle's trajectory together with the corresponding covariance matrix estimated at a given point in space.

First a local reconstruction of clusters is performed in each detector. Then vertexes and tracks are reconstructed and particles types are identified. The output of the reconstruction is the Event Summary Data (ESD).^[3]

4. Clustering method (TRD)

The currently employed clustering mechanism searches for adjacent pads in y-direction with a signal above threshold that could form a pad cluster. Since there is only little charge sharing in z-direction no clustering

is performed here. The same is true for the drift direction, since a track, due to the high ionization in Xe, creates a signal in basically every time bin. Therefore the position of a cluster in z - and drift direction is determined by the pad and time bin position. The position in y -direction, where a good resolution is mandatory for the momentum measurement, can be extracted with much higher precision, due to the charge sharing. Here one can either calculate the center of gravity of the charge distribution inside a cluster, or use a lookup table to determine the position of the cluster. The latter method, where the position is taken from a table that contains the deviation from the pad center as a function of the ratio of the two largest signals provides generally a better resolution.

Ideally, all clusters contain only signals from two or three pads (2.4 on average for an isolated hit). In the high multiplicity environment of the ALICE experiment, however, there is a large probability that clusters overlap. Currently, only clusters containing signals from five pads are unfolded, using the pad response function as an estimator for the cluster shape. By applying a more sophisticated mechanism one also can disentangle clusters composed of 4 and more pads, thereby reaching a further improvement in resolution at high multiplicity.

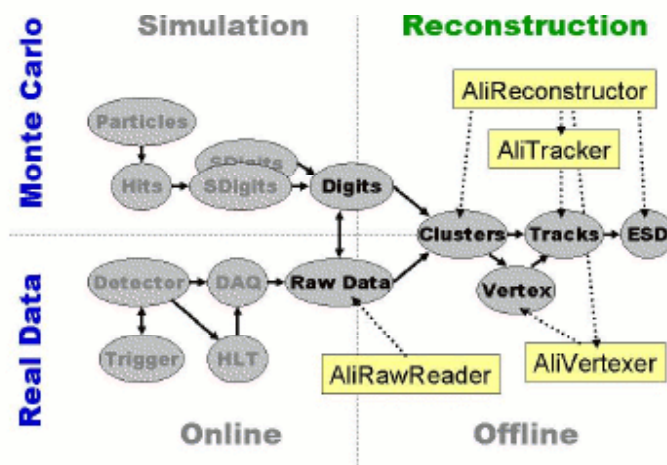
5. Tracking and PID

The TRD tracking is an important component of ALICE barrel tracking in adding level arm to the tracks found by Time Projection Chamber (TPC) detector and thus improving

momentum resolution. Additionally it is the starting point for the algorithm of Particle IDentification (PID). For each TRD chamber, cluster are reconstructed as described. Based on tracking seeds clusters are grouped and linear fits are performed on them on a chamber by chamber basis. The parameters of the linear fits are describing the so called "tracklets". The last step in buiding the TRD segment of an ALICE track is to fit such tracklets based on a detailed description of the magnetic field and material budget. Here the Kalman filter algorithm is used.

For starting (seeding) tracks in TRD two methods are currently employed. The first which works in the large majority of cases is to use tracks from TPC as seeds. The second method is auto (stand alone) seeding by discovering topological correlations between clusters in one stack. This second method is of particular use in tracking conversion electrons generated after TPC or in reconstructing runs in which TRD is not helped by TPC (cosmic or calibration runs).

The PID calculation is based on comparing energy loss measurements along a track with reference data. To exploit the high granularity of detection along track (time granularity) several multidimensional methods have been developed based on algorithm such ass Neural Networks, Likelihood estimators and Local Interpolators. The performance of such algoritms can reduce the pion background up to orders of 0.1%^[1].



AliEve is ALICE Event Visualization Environment. It is built on top of ROOT's EVE module which in turn uses ROOT's GUI and OpenGL functionality.

It provides the user a visualization of reconstructed events.

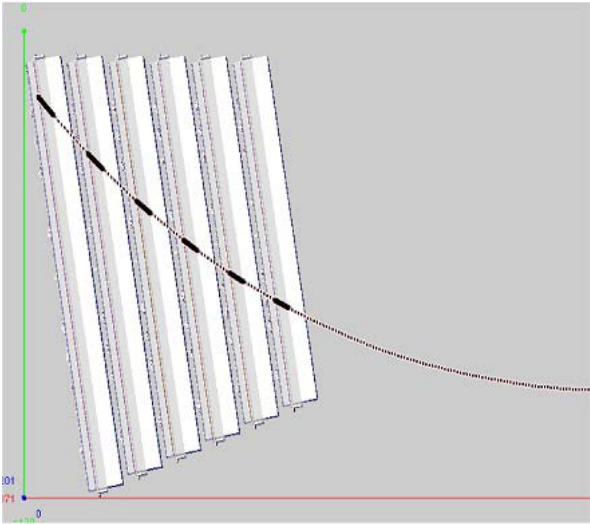


Fig. 2 TRD detector stack, simulated MC track and the detector "hits"

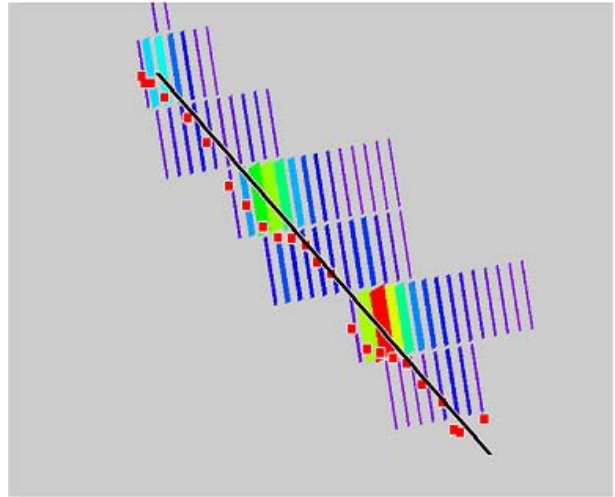


Fig. 4 the Tracklet is rendered as a linear fit of the clusters.

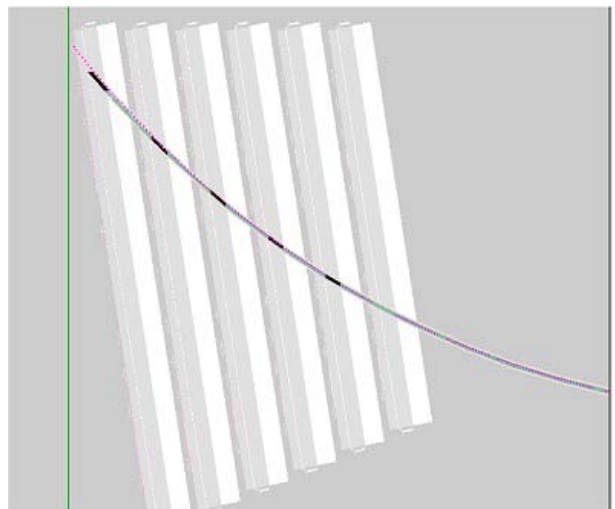


Fig. 5 Reconstructed track with corresponding tracklets rendered together with the MonteCarlo simulated track.

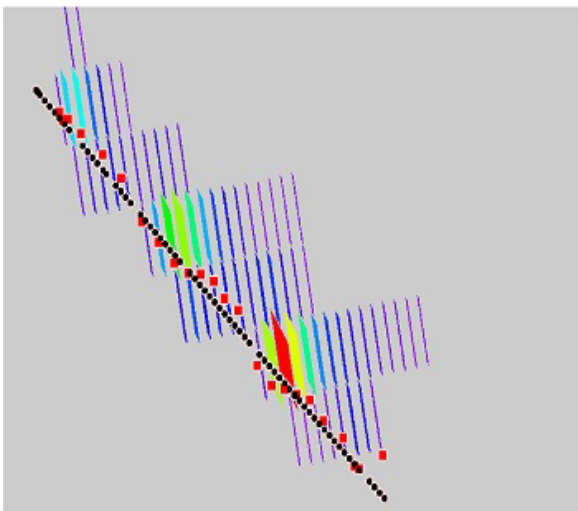
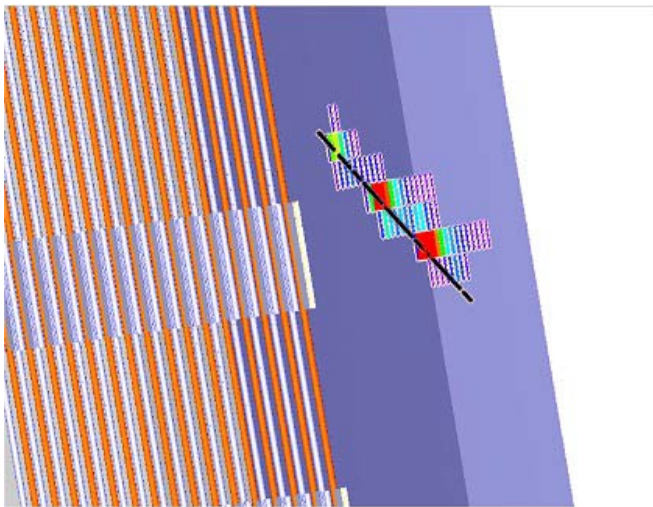


Fig. 3 The clusters are rendered and calculated using the method outlined above

6. Conclusion

While working on the visualization of digits and tracks , I've come to believe that the reconstruction methods outlined above are accurate within an acceptable margin or error and that this error can be steadily decreased as the methods are being improved.

7. References

- [1] Alice Tehnical Design Report of the transition radiation detector, CERN/LHC 2001-021, ALICE TRD 9, 3 OCT 2001
- [2] Alice: Phisics Performance report, Volume I, Ed. Alice Collaboration, Published 19 OCT 2004
- [3] AliROOT documentation aliweb.cern.ch

Students program

Date & hour	Title of the presentation	Speaker
We, July 7 13:00 - 15:00	Detection & Identification methods in Nuclear and Particle Physics Experiments	Mihai
Fr, July 9 9:00 - 10:30	Introduction to Monte-Carlo simulations	Ionela
Mo, July 12 13:00 - 15:00	Introduction to ALICE-TRD concept & calibration	Alexandru
We, July 14 13:00 - 14:30	RPC - general presentation	Mariana
Fr, July 16 11:30 - 13:00	Heavy Ion Collisions - Introduction to Phenomenological Models	Dan
Mo, July 19 13:00 - 15:00	Physics analysis based on AliROOT	Andrei and Cristi
Tue, July 20 13:00 - 14:30	CADENCE for pedestrians	Puiu
We, July 21 13:00 - 15:00	Heavy Ion Collisions at Intermediate Energies	Amalia
Th, July 22 13:00 - 14:30	Introduction to Nuclear Electronics	Cara, Bugi
Fr, July 23 8:30 - 10:00	GRID concept and implementation	Claudiu



In these 3 weeks I've learned how particle detectors are built up – a new chapter in my experience, and that theory without practice is dead and practice without theory is blind.

D.C.

To be here at IFIN-HH means to finally get the chance to meet and work with the best people in the field, and learn from them as much as possible. It is a chance to figure out the future in terms of “what would you like to be when you grow up”.

M.T.

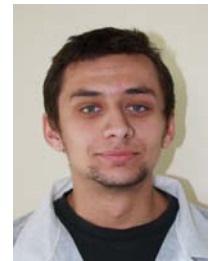


A bright experience that surely will be useful in my long waited, hopefully, successful career. For three weeks we were physicists without any documents to prove it.

C.V.

An interesting and unique experience which offered an insight in particle physics experiments and applied research.

S.T.



During my stay here, I've learned more about the interface between experiment and theory in very large experiments. Event reconstruction provides an unique insight into the underlying problems and challenges of such a project.

M.P.



During the 3 weeks of our stay here we have met a whole new world, the one of hadronics. Curious to know where everything has started, we gave a hand to science and understood the process of revealing some of the secrets of the Universe: how to transform invisible physical phenomena into visible understandable data using detectors and data acquisition systems. Also we encountered a great team of scientists dedicated to their work that showed us how to understand and love science and guided us throughout the period of time.

I.P. & A.S.



Regards

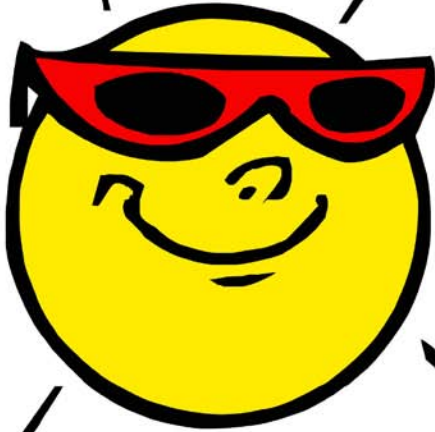
“To the staff that allowed us to enter into their home and played with their toys – patiently stayed by us step by step and shared a bit of their knowledge.

And to the ones that made this possible.”

The students



And finally we had fun...



IFIN-HH

You are all invited

DFH building

Friday, 23
12:00

Team building break, bring the fun we cover the rest:

Barbeque, drinks, and a great time.

DFH

STUDENT SUMMER PARTY!

DFH

The graphic features a central yellow smiley face with red sunglasses. Above it is a banner of colorful balloons and streamers with the text 'You are all invited'. To the left, 'DFH building' and 'Friday, 23 12:00' are listed. To the right, two lines of text describe the event: 'Team building break, bring the fun we cover the rest:' and 'Barbeque, drinks, and a great time.'. The top and bottom of the graphic are framed by 'IFIN-HH' and 'DFH' logos respectively, with the bottom text 'STUDENT SUMMER PARTY!' set against a grass background.



Horia Hulubei - National Institute for Physics and Nuclear Engineering (NIPNE), Bucharest
Hadronic Physics Department

Address: Str. Atomistilor no.407, P.O.BOX MG-6, Bucharest - Magurele, ROMANIA

<http://niham.nipne.ro>
phone: 0040-21-4042392
fax: 0040-21-4574432

